
**Crull, K., Rohde, M., Westphal, K., Loessner, H., Wolf, K., Felipe-López, A., Hensel, M., Weiss, S.**

**Biofilm formation by salmonella enterica serovar typhimurium colonizing solid tumours**

**(2011) Cellular Microbiology, 13 (8), pp. 1223-1233**

Cellular Microbiology (2011) **13**(8), 1223–1233
doi:10.1111/j.1462-5822.2011.01612.x
First published online 25 May 2011

# Biofilm formation by *Salmonella enterica* serovar Typhimurium colonizing solid tumours

**Katja Crull,[1]* Manfred Rohde,[2] Kathrin Westphal,[1] Holger Loessner,[1,3] Kathrin Wolf,[1] Alfonso Felipe-López,[4] Michael Hensel[4] and Siegfried Weiss[1]**

[1]*Molecular Immunology, HZI – Helmholtz Centre for Infection Research, Inhoffenstr. 7, D-38124 Braunschweig, Germany.*
[2]*Medical Microbiology, HZI – Helmholtz Centre for Infection Research, Inhoffenstr. 7, D-38124 Braunschweig, Germany.*
[3]*Veterinary Department, Paul-Ehrlich-Institute, Paul-Ehrlich-Str. 51-59, D-63225 Langen, Germany.*
[4]*Division Microbiology, University of Osnabrück, Barbarastraße 11, D-49076, Osnabrück, Germany.*

## Summary

**Systemic administration of *Salmonella enterica* serovar Typhimurium to tumour bearing mice results in preferential colonization of the tumours and retardation of tumour growth. Although the bacteria are able to invade the tumour cells *in vitro*, in tumours they were never detected intracellularly. Ultrastructural analysis of *Salmonella*-colonized tumours revealed that the bacteria had formed biofilms. Interestingly, depletion of neutrophilic granulocytes drastically reduced biofilm formation. Obviously, bacteria form biofilms in response to the immune reactions of the host. Importantly, we tested *Salmonella* mutants that were no longer able to form biofilms by deleting central regulators of biofilm formation. Such bacteria could be observed intracellularly in immune cells of the host or in tumour cells. Thus, tumour colonizing *S. typhimurium* might form biofilms as protection against phagocytosis. Since other bacteria are behaving similarly, solid murine tumours might represent a unique model to study biofilm formation *in vivo*.**

## Introduction

The observation that solid tumours are treatable via bacterial infection was made a considerable time ago (Coley, 1893; Hoption Cann *et al*., 2003) and might even date back to ancient Egypt (Ebbell, 1937). Quite a number of bacterial species have now been shown to preferentially colonize cancerous tissue as compared with the healthy organs when applied systemically to tumour bearing mice (Leschner and Weiss, 2010). Bacterial colonization of tumours could result in retardation of growth or even complete clearance of the tumour. Accordingly, tumour targeting using bacteria is currently a matter of intensive research.

*Salmonella enterica* serovar Typhimurium (*S. typhimurium*) is one of the bacterial species that is intensively investigated for its potential to treat tumours. First clinical trials using highly attenuated *S. typhimurium* variants have been reported (Cunningham and Nemunaitis, 2001). These bacteria were suggested to actively force tumour entry by inducing a cytokine storm when applied intravenously. Induction of cytokines like TNF-$\alpha$ results in the disruption of the pathological endothelia of the blood vessels in the tumour with a subsequent haemorrhage that flushes in the bacteria (Leschner *et al*., 2009). The necrosis caused by the haemorrhage generates a microenvironment in which the bacteria can thrive. At the same time, neutrophilic granulocytes are attracted to the tumour. Those phagocytes form a physical barrier that restricts the bacteria to the necrotic areas (Westphal *et al*., 2008). Originally, we attributed the inability of these neutrophils to phagocytose the bacteria to the low concentration of oxygen in such tumour regions. Now we show that the bacteria produce biofilms in response to host neutrophils that protect them from up-take by phagocytic as well as tumour cells.

Biofilms are sessile communities of bacteria. They can be formed by single or multiple bacterial species and might even include fungi or yeast (Hoiby *et al*., 2010; Loussert *et al*., 2010). The bacteria are either attached to each other or to surfaces by expressing specific adhesion molecule (Scher *et al*., 2005; White *et al*., 2006). In addition, they produce an extracellular, polymeric and highly heterogenous and variable matrix. Components can include polysaccharides, proteins, glycoproteins and glycolipids, in rare cases even extracellular DNA (Dickschat, 2010; Flemming and Wingender, 2010). The individual consistency of the extracellular matrix depends on the bacterial strain or strain combinations as well as growth and environmental conditions. Besides providing

Received 19 January, 2011; revised 12 April, 2011; accepted 13 April, 2011. *For correspondence. E-mail kko07@helmholtz-hzi.de; Tel. (+49) 531 6181 5113; Fax (+49) 531 6181 5002.

advantages in capturing environmental nutrients, the main function of biofilms is to provide a physical barrier (Shirtliff *et al*., 2002; Hall-Stoodley and Stoodley, 2005). Bacteria in such biofilms can hardly be reached by assaults from the environment or antimicrobial substances.

*Salmonella typhimurium* is known to be able to produce biofilms on glass and plastic surfaces (Stepanovic *et al*., 2004) as well as on gallstones (Crawford *et al*., 2010). Especially *in vitro*, biofilm formation of *S. typhimurium* has been intensively investigated (McBain, 2009). Cellulose has been identified as main exopolysaccharide on abiotic glass surfaces in contrast to gallstones (Scher *et al*., 2005).

Most wild-type *S. typhimurium* strains exhibit the formation of red, dry and rough colonies on Congo red (CR) agar plates called the 'rdar' morphotype that might be synonymous to the formation of biofilms (Simm *et al*., 2007). Besides cellulose, intact curli fimbriae are required for this morphotype as the hydrophobic dye CR is bound by highly adhesive, amyloid curli fibres. Production of curli fimbriae is tightly regulated. *In vitro*, curli production occurs at temperatures below 30°C. Higher temperatures induce formation of white and smooth colonies on CR agar plates due to the absence of curli (Römling *et al*., 1998; White *et al*., 2003; Jonas *et al*., 2007). Expression of curli is positively regulated via transcriptional activation of the structural genes *csgBAC* by the major biofilm regulator *csgD.* In addition, *csgD* is indirectly involved in cellulose production via activation of *adrA* (Römling *et al*., 1998; Gerstel and Römling, 2003; Gualdi *et al*., 2007). In turn, *adrA* activates one or more products of the *bcsABZC–bcsEFG* operons via posttranscriptional activation through the secondary messenger c-di-GMP. Those operons encode the structural genes for cellulose biosynthesis. However, cellulose might also be produced independent of *csgD* via activation by an alternative di-guanylate cyclase (Römling, 2005).

In the present work, we demonstrate that *S. typhimurium* when colonizing solid, murine tumours forms biofilms as protection against phagocytosis by host immune cells. This explains why such bacteria are found exclusively extracellularly in tumours. In accordance, bacterial mutants that were unable to form biofilms were found to reside in phagocytes or tumour cells.

## Results

### S. typhimurium *is able to invade CT26 cells* in vitro

In our previous work we had never found intracellularly residing *S. typhimurium* SL7207 when colonizing CT26 tumours *in vivo*. However, *S. typhimurium* is able to invade non-phagocytic cells by injecting virulence factors into host cells via the *Salmonella* pathogenicity island 1-encoded type three secretion system (TTSS), which triggers cytoskeleton rearrangements to induce macropinocytosis (Lahiri *et al*., 2010). Hence, we wanted to know whether SL7207 is able to invade CT26 cells under *in vitro* conditions. To answer this question, *S. typhimurium* SL7207 was added to CT26 cells in culture with a multiplicity of infection (moi) of 100 and 2 h post infection (p.i.) Z-stack pictures were taken using confocal microscopy to demonstrate the presence of intracellular bacteria. We could confirm that SL7207 is able to invade CT26 cells with a low efficacy (2% of the inoculum) since single bacteria could be found within the CT26 cells (Fig. S1A).

This was corroborated by adding gentamicin to the cultures 2 h p.i. Since gentamicin is not membrane permeable, intracellular bacteria should be protected. Indeed, gentamicin protected bacteria could be found confirming that SL7207 was able to invade CT26 cells with a low efficacy. As a control, the non-invasive *E. coli* Nissle (EcN), when tested in the gentamicin protection assay, was not able to form colonies on plates after gentamicin treatment (Fig. S1B).

### *In solid CT26 tumours* S. typhimurium *SL7207 resides extracellularly and forms biofilm-like structures*

So far, extracellular residence of tumour colonizing *S. typhimurium* was based on suggestive evidence provided by various histological findings. Since bacteria were found intracellularly under *in vitro* conditions, we wanted to compellingly exclude by ultrastructural analysis that tumour colonizing *Salmonella* reside intracellularly.

Transmission electron microscopy of tumours 2 days p.i. revealed that the bacteria could be found in small colonies and resided extracellularly (Fig. 1). Importantly, the bacteria were embedded in an electron-dense, extracellular material, most probably an extracellular polymeric matrix. The appearance of this material resembles earlier observations when extracellular matrix material during biofilm formation was examined on ultrathin sections (Römling and Rohde, 1999; Römling *et al*., 2000). In addition, plasmolysis of the bacteria could be detected (Fig. 1, left panels: asterisks). Plasmolysis can be taken as an indication of bacterial stress.

Scanning electron micrographs revealed the extracellular matrix even more clearly. It also confirmed that salmonellae are not equally distributed throughout the hypoxic/necrotic parts of the tumour but form colonies at distinct places. In such areas, sheath-like structures (Fig. 1, right panels) can be found that apparently were embedding the bacteria. Such structures had been observed before when investigating biofilm formation of *S. typhimurium in vitro* (Römling and Rohde, 1999; Römling *et al*., 2000).

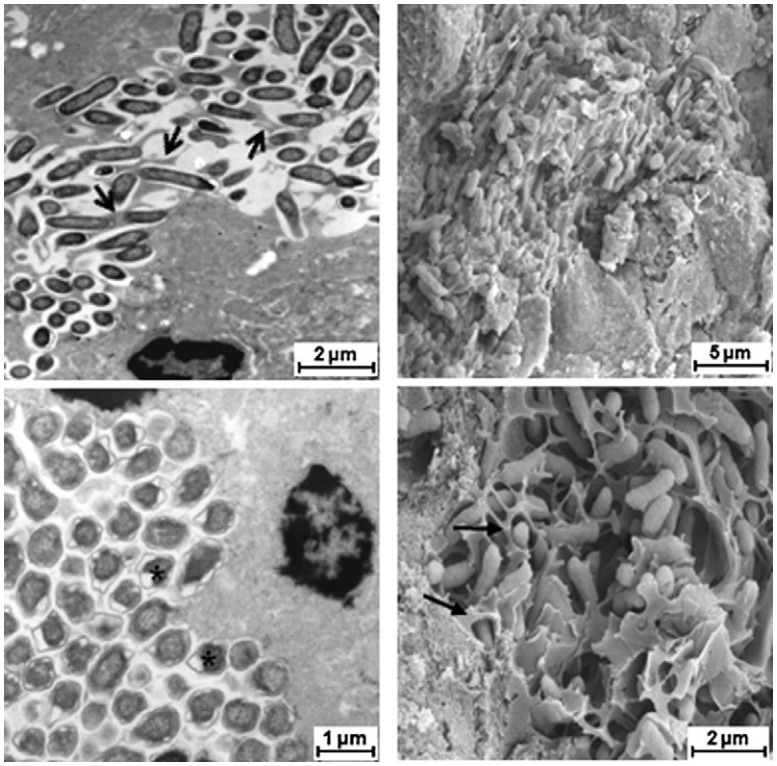


**Fig. 1.** Transmission electron microscopy images and scanning electron micrographs of CT26 tumours 2 days after application of *S. typhimurium* SL7207. Bacteria are embedded in electron dense material (left top panel: arrows) indicating biofilm formation. Sheet-like structures in right panels (arrows) also indicate biofilm formation. Severe plasmolysis is observed in such bacteria (left bottom panel: asterisks).

The extracellular residence of the tumour colonizing bacteria was confirmed using the *ex vivo* gentamicin protection assay (Avogadri *et al*., 2005). CT26 tumour-bearing mice were intravenously infected with $5 \times 10^6$ *S. typhimurium* SL7207. Tumours were taken 2 days p.i. and organ homogenates were treated with gentamicin (Fig. 2). Only about 20% of the SL7207 bacteria were resistant to gentamicin i.e. possibly residing intracellularly. The same pattern has been observed for spleen. As a control, the tumour-colonizing *E. coli* Nissle strain showed no resistance to the *ex vivo* gentamicin treatment. Due to the lack of pathogenicity factors like TTSS, *E. coli* Nissle is non-invasive and should remain extracellularly in the tumour.

### *Specific expression of csgD in tumour colonizing* S. typhimurium *SL7207*

Biofilms defined for *S. typhimurium in vitro* consisted mainly of curli fimbria and cellulose as extracellular polymers (Römling and Rohde, 1999; Römling *et al*., 2000). We therefore wanted to test whether such components were also involved in biofilm formation in tumours. Thus, we determined the RNA expression levels for the constitutively expressed *bcsA* gene and the regulated genes *adrA* and *csgD.* Such genes directly or indirectly regulate biosynthesis of cellulose and curli fimbria. RT-PCR and qPCR revealed that in the untreated, infected tumour the expression level of *bcsA* is as high as the housekeeping gene *gyrB*. In contrast, for *adrA* and *csgD,* both regulators of biofilms, involved in cellulose production and curli fimbriae, a higher expression is found in the untreated tumour (Fig. 3A). In confirmation, similar data are obtained, when *Salmonella* grown on appropriate plates at 30°C or 37°C are compared (Fig. 3C). While *bscA* and *ardA* yielded almost equal ratios to the house keeping gene under both conditions, the major regulator *csgD* is clearly lower at the none biofilm supporting condition. This suggests that biofilms formed by *S. typhimurium* in tumours are similar to those observed *in vitro*.

### *Biofilm formation by* S. typhimurium *in tumours is a reaction against immune cells of the host*

Tumour colonizing *S. typhimurium* could form biofilms for example for efficient capturing of nutrients or as a defence reaction against immune cells of the host. Since under our conditions the most prominent immune cells in colonized CT26 tumours are neutrophilic granulocytes, we depleted such cells by treating mice three times with an anti-Gr1 antibody during infection. Two days p.i., the tumours were removed and analysed by electron microscopy (Fig. 4). Most remarkably, transmission electron microscopy revealed dramatically reduced formation of extracellular matrix, even though minimal electron dense material and extracellular structures are still visible. Furthermore, the level of plasmolysis is decreased compared with the

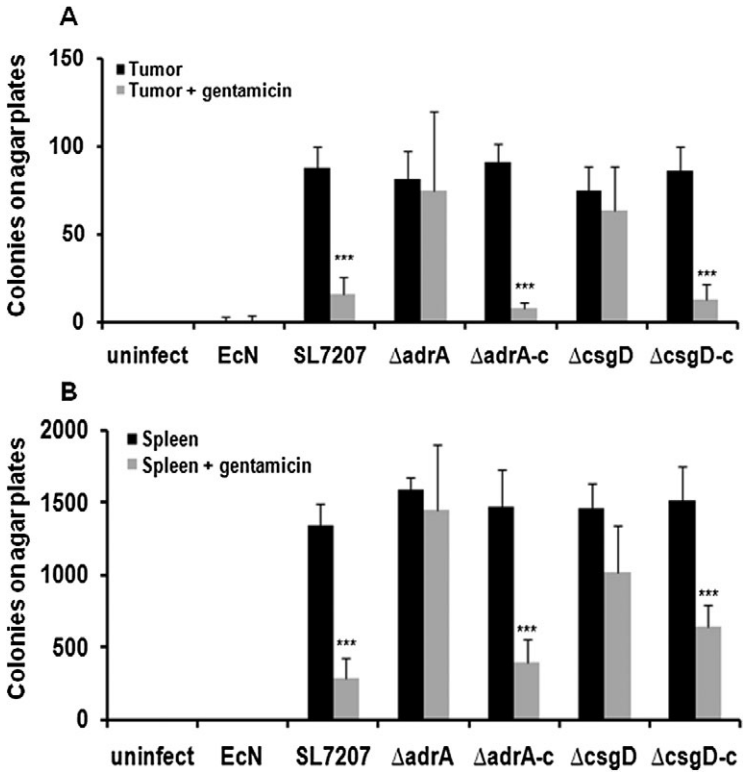


**Fig. 2.** *Ex vivo* gentamicin protection assay. Tumour bearing mice were infected with the various strains including *E. coli* Nissle 1917 (EcN). Two days later tumours (A) and spleens (B) were homogenized, treated with gentamicin and plated. Mean cfu values of 4 replicates are shown with standard deviations. Statistical significance (*) was calculated using Student's *t*-test by showing cfu of the various strains after gentamicin addition compared with samples without gentamicin treatment. ***$P < 0.001$.

none-depleted control. This suggests that biofilm formation is induced as a response against immune cells of the host, most likely the activity of neutrophilic granulocytes.

To corroborate these findings, we tested the expression of bacterial genes involved in biofilm formation in the tumour after depletion of granulocytes. Real-time PCR was performed using bacterial RNA from colonized tumours after anti-Gr1 treatment. Again, the constitutively expressed *bcsA* was expressed like the housekeeping gene *gyrB*. However, the expression levels of *csgD* and *adrA* were clearly decreased compared with the control (Fig. 3A). This is even more apparent when the bacterial RNA from normal colonized tumours and tumours after depletion of neutrophilic granulocytes is compared. Clearly, expression of *Salmonella* genes, controlling biofilm formation, is significantly downregulated in neutrophil-depleted mice (Fig. 3B). This confirms the results obtained by electron microscopy.

### S. typhimurium *SL7207 mutants unable to form biofilms can be found intracellularly*

To learn more about the function of biofilm formation by tumour colonizing *S. typhimurium* SL7207, we generated deletion mutants for *adrA* (Δ*adrA*) and *csgD* (Δ*csgD*) and tested the relevance of those genes first *in vitro*. Obviously, both variants were no longer able to form the typical biofilm i.e. the 'rdar' morphotype *in vitro*. While SL7207 was able to form rough colonies, the mutants SL7207Δ*adrA* and SL7207Δ*csgD* were not (Fig. 5A). In addition, as revealed by staining colonies with Calcofluor both variants were hardly able to synthesize cellulose in contrast to the parental strain (Fig. 5B). Importantly, the phenotype of cellulose-containing, rough colonies could be restored by complementing the mutations with plasmids constitutively expressing *adrA* (Δ*adrA*-c) and *csgD* (Δ*csgD*-c) respectively (Fig. 5A and B). Interestingly, the up-take of the mutant and their complemented counterparts were equally invasive for CT26 *in vitro*. Obviously, under *in vitro* conditions the ability to form biofilms does not play a role for host cell invasion (Fig. S1B).

Since those mutants showed the expected phenotype *in vitro* on biofilm plates, we proceeded to test them *in vivo.* Thus, CT26 tumour bearing mice were infected with either SL7207, the mutant strains Δ*adrA or* Δ*csgD,* or the complemented strains Δ*adrA*-c and Δ*csgD*-c. Two days p.i., colonized tumours were analysed by transmission electron microscopy. Most remarkably, in contrast to SL7207 bacteria, which reside exclusively extracellularly and form biofilms, both variant bacteria could be found intracellularly (Fig. 5C, magnifications Fig. S2). Bacteria reside in either small cells that could represent neutrophilic granulocytes as depicted for the Δ*adrA* mutant or they reside in large cells as depicted for the Δ*csgD* variant that most likely represent tumour cells. Still, definition of the infected cells needs more detailed clarification.

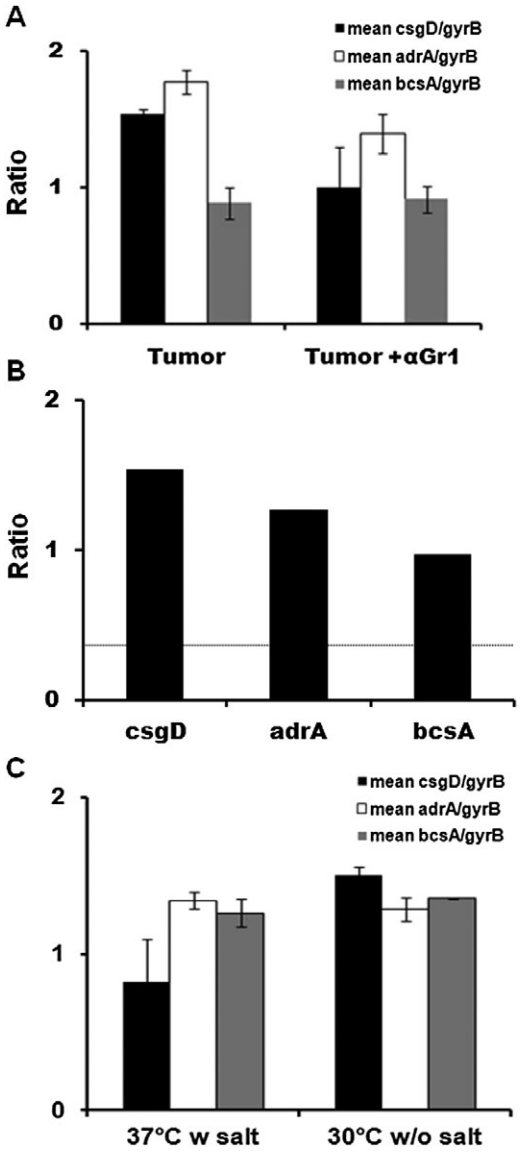


**Fig. 3.** Expression of genes associated with biofilm formation by tumour colonizing *S. typhimurium SL7207*.
A. Gene expression of SL7207 from untreated tumour samples and tumours from mice after anti-Gr1 (α-Gr1) depletion. The expression level ratio of the particular gene in relationship to the housekeeping gene (*gyrB*) is shown. Bars represent the mean of 3 biological replicates with standard deviations.
B. Relative bacterial gene expression levels (depicted in A) of untreated tumours in relationship to neutrophil-depleted tumours.
C. As *in vitro* control, the ratios of particular bacterial gene expression levels in relationship to expression levels of *gyrB* is shown. Samples were derived either from biofilm plates incubated at 30°C or LB plates incubated at 37°C.

The complemented strains can no longer be found intracellularly (Fig. 5C, magnifications Fig. S2). This was accompanied by restored biofilm formation. Those findings were supported by results of the *ex vivo* gentamicin protection assay. For SL7207Δ*adrA* and SL7207Δ*csgD* a higher number of bacteria were resistant to gentamicin and thus reside intracellularly (Fig. 2).

### *Biofilms of* S. typhimurium *are formed between necrotic areas and the viable rim of CT26 tumours*

Tumour colonizing *S. typhimurium* reside in the necrotic areas of the tumour and in the areas where the necrotic region borders the remaining viable rim (Loessner *et al*., 2007). This localization overlaps slightly with the barrier formed by neutrophilic granulocytes (Westphal *et al*., 2008). In these regions, the bacteria are most concentrated and biofilm formation is most likely to take place there. Staining paraffin sections from colonized tumours for glycogens using the PAS method revealed that indeed biofilms are especially formed at the predicted area between viable rim and necrotic regions (Fig. 6, magnifications Fig. S3). Prominent strong signals were found at particular spots (Fig. 6, arrows). Importantly, PAS-positive staining was almost only found for the parental strain as well as for the complemented strains but was hardly detectable when tumours were colonized by the mutant strains (Fig. 6, magnifications Fig. S3). This, first of all, indicates the specificity of the assay and second, that biofilms are formed where bacteria are most concentrated, as indicated by the concentrated glycogens at this region.

### S. typhimurium *SL7207 mutants unable to form biofilms show reduced therapeutic potential*

The mutations of *adrA* and *csgD* might not only affect biofilm formation but also additional functions. We therefore wanted to test the performance of such variants in an *in vivo* tumour targeting experiment. As Fig. S4A demonstrates, both mutants show reduced tumour invasion efficiency compared with the parental strain. Only after 48 h the bacterial colonization has recovered to counts similar to SL7207. Similarly, spleen and liver colonization by the variants was slightly reduced. Taken together, this obviously has consequences on the therapeutic potential. Only some tumours were cleared by the Δ*adrA* variant and the Δ*csgD* variant was unable to clear any of the tumours. In contrast, the parental bacteria were able to clear all CT26 tumours (Fig. S4B).

## Discussion

The *S. typhimurium* strain SL7207 has been used for several studies on bacterial tumour colonization (Yu *et al*., 2004; Royo *et al*., 2007; Stritzker *et al*., 2010). Here we report a novel feature of this strain when residing in tumours – namely the formation of biofilms. Ultrastructural analysis revealed that the bacteria were apparently

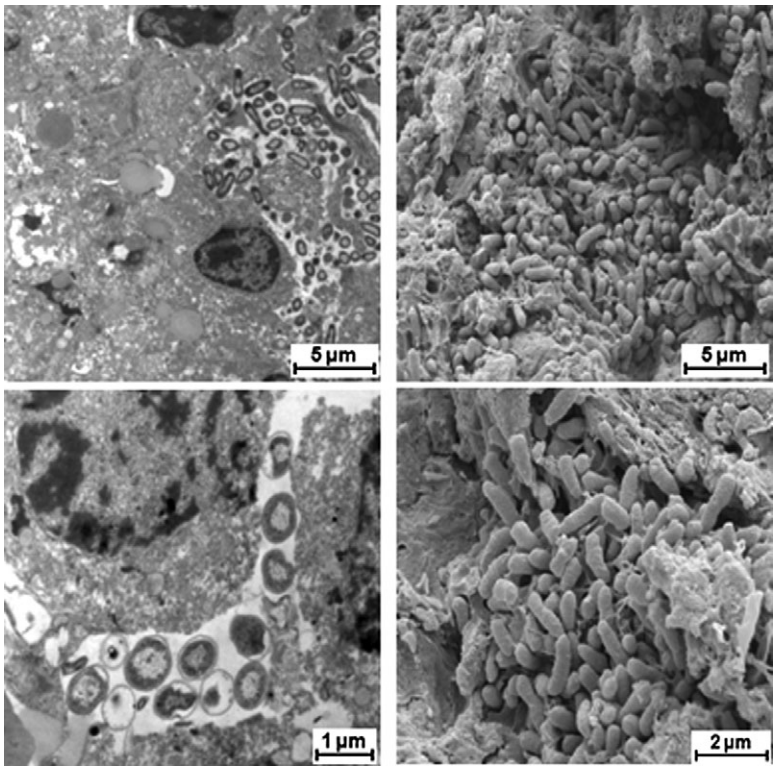


**Fig. 4.** Transmission electron microscopy images and scanning electron micrographs of CT26 tumours 2 days after infection with *S. typhimurium* SL7207. Depletion of neutrophilic granulocytes was achieved by injecting anti-Gr1 at day −1, 0 (day of infection) and 1. Only a minor extend of biofilm formation can be observed. Plasmolysis was also strongly reduced.

embedded in an extracellular matrix. Such structures were reminiscent of the biofilms formed *in vitro* that had been extensively characterized by Römling *et al*. (Römling, 2005; Jonas *et al*., 2007; Grantcharova *et al*., 2010).

In such studies, the central switch for biofilm formation was identified as *csgD*. It drives expression of the structural genes of curli fimbriae and activates *adrA*, which in turn activates the synthetase for cellulose. The expression pattern of such bacterial genes in the tumour is in accordance with this. While *bscA* and *bcsB* the structural genes of cellulose synthetase are constitutively expressed, as expected, *csgD* and *adrA* are rigorously regulated and strongly expressed in tumour residing bacteria.

Transcription of the major regulator *csgD* is induced by a number of environmental stimuli like low temperature, low oxygen tension, low osmolarity and low pH. Several of these conditions might be encountered when the bacteria reside in the tumour. However, additional key signals must be received under these conditions. Obviously, the bacteria are severely stressed since many of them show plasmolysis. In addition, depletion of neutrophils reduces the extend of plasmolysis as well as the formation of biofilms. This indicates that biofilm formation by the bacteria is, to a large extend, a reaction against the neutrophils of the host that are attracted to the tumour after colonization (Westphal *et al*., 2008). Substances produced by such neutrophils might provide additional triggers for bacterial aggregation and the formation of an extracellular matrix. Such substances could be small molecules released by the neutrophils like oxygen radicals or hypochlorite but also defensin-like bactericidal substances. Defensins have been shown to also trigger bacterial reactions via the *phoP*/*phoQ* pathway (Lehrer, 2004). A similar scenario can be envisioned for *csgD*.

Biofilm formation now explains the puzzling finding that *S. typhimurium* in the tumour is almost never found intracellular (Loessner *et al*., 2007). However, as soon as we interfere with the ability of *Salmonella* to produce biofilms, bacteria are found intracellularly. Although it is not possible by our ultrastructural analysis to define the cells in which the bacteria reside, their size suggests that tumour cells as well as neutrophils have taken up bacteria.

The involvement of *csgD* and *adrA* suggests that the composition of biofilms formed by *S. typhimurium* in solid tumours is similar to the biofilms observed for such bacteria *in vitro*. The bacteria are highly aggregated in the areas between necrosis and the viable rim. Only this area can be stained for glycogens. Nevertheless, further research will be required to definitely show the involvement of curli and cellulose. For instance, appropriate mutants could be tested.

Delayed tumour colonization was observed for the two variants. This could be due to their inability to form biofilms. Thus, the bacteria might be vulnerable toward host immune cells. On the other hand, *csgD* and *adrA* are

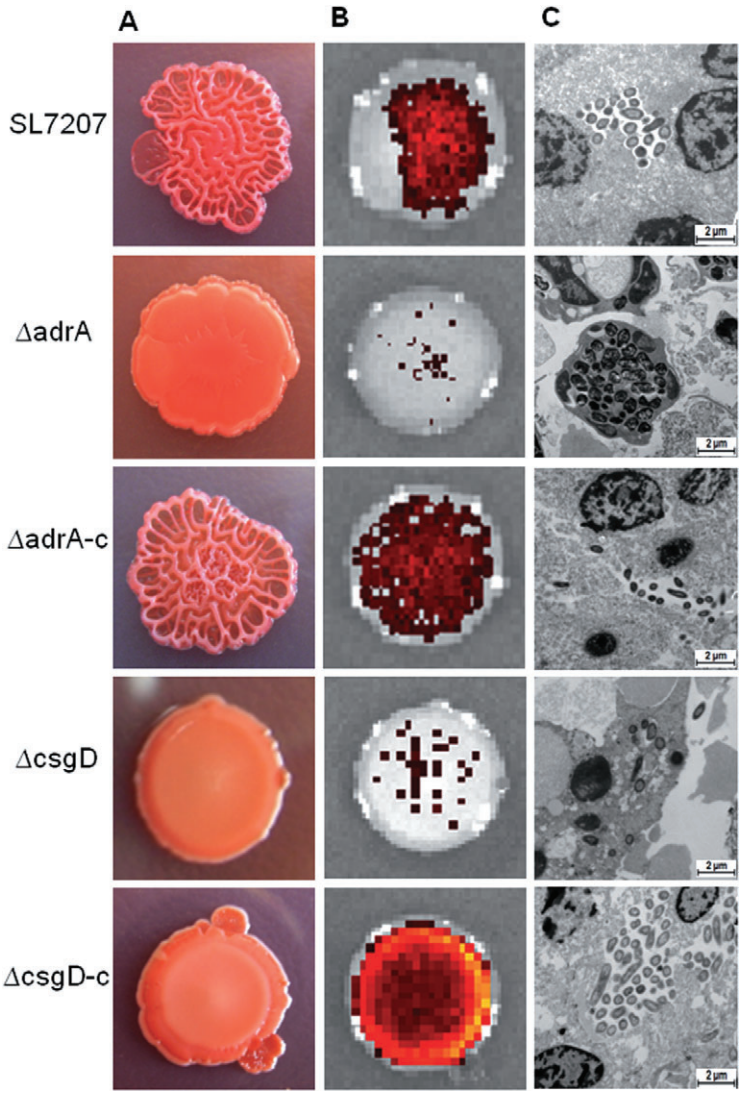


**Fig. 5.** Biofilm formation of *S. typhimurium*.
A. Colonies on salt-free CR agar plates incubated at 30°C show the rdar morphotype.
B. Fluorescence of Calcofluor as indicator for cellulose in S. *typhimurium* biofilms on CR agar plates.
C. Transmission electron micrographs of CT26 tumours resected 2 days post infection (see Fig. S2 for enlarged pictures).

pleiotropic regulators and we can presently not exclude that some of such functions might be necessary for *in vivo* survival and tumour targeting. Consequently the therapeutic potential was impaired (Fig. S4). However, intracellular bacteria might now allow more efficient usage of alternative therapeutic strategies. For instance, we believe that the extracellular residence of the bacteria in tumours restricted their potential to act as gene transfer vehicles. This might be circumvented now by employing appropriate mutants. Thus, from our finding novel strategies for cancer therapy might be developed.

Many bacteria have the property to form biofilms. This poses serious problems in the clinics. Often, medical devices are contaminated in the patient by bacteria that form biofilms. In addition, biotic surfaces such as cardiac valves might be incapacitated by biofilms derived from bacteria. The most severe complication due to bacterial biofilms is encountered in the lungs of patients suffering from cystic fibrosis. This renders the bacteria insensitive to antibiotics and finally leads to the death of the patient. Therefore, *in vivo* investigations on biofilm formation is a major challenge for modern biomedical research. However, very few appropriate *in vivo* models are presently available. Studies on biofilm formation by bacteria in tumours might be able to fill this gap.

## Experimental procedures

### *Bacterial strains and growth conditions*

*Salmonella typhimurium* strain SL7207 (Δ*hisG*, Δ*aroA*) was kindly provided by Bruce Stocker (Hoiseth and Stocker, 1981). The deletion mutant strain SL7207Δ*adrA* was generated by PCR-driven deletion (Datsenko and Wanner, 2000). In SL7207Δ*adrA-c* the deletion was complemented by expressing *adrA* from the low-copy number plasmid pMB1 under the $P_{bla}$ promoter (Loessner *et al.*, 2007). The same procedure was followed for

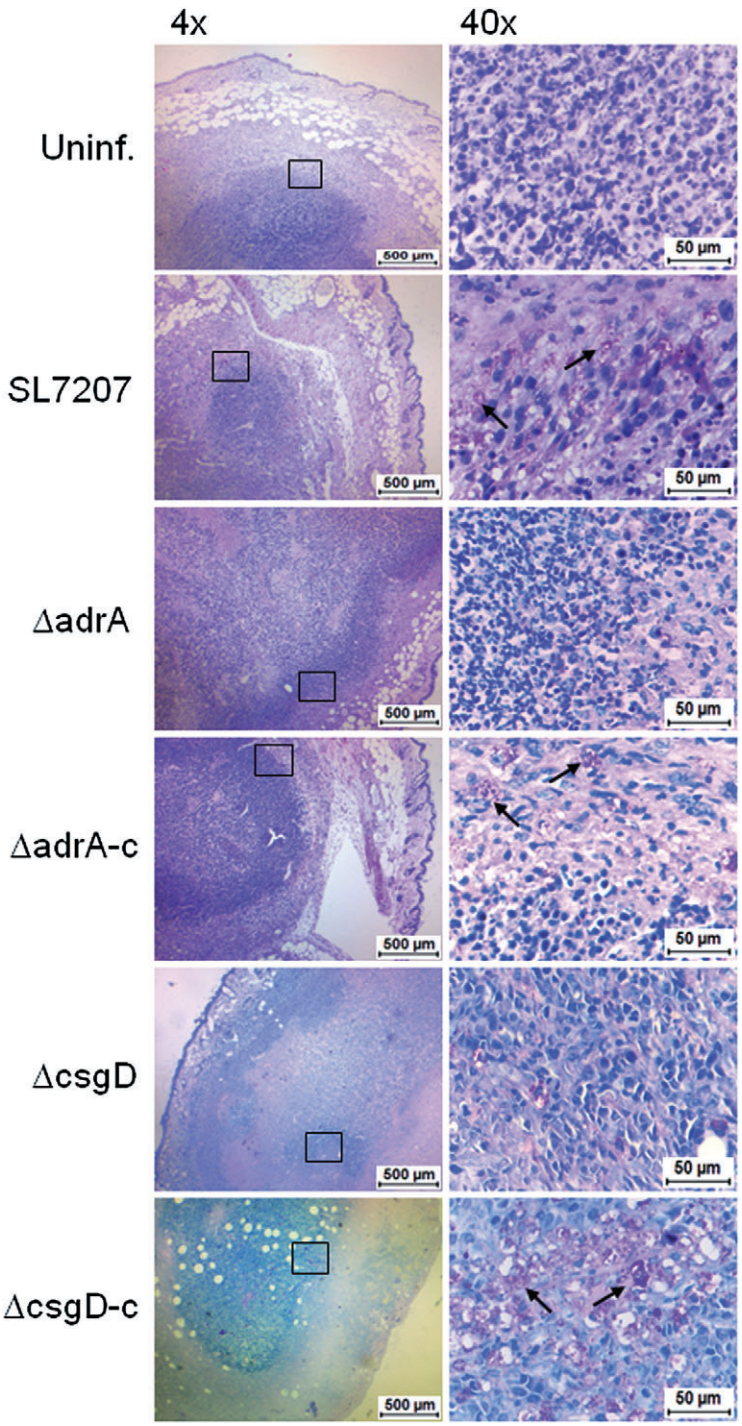


**Fig. 6.** PAS staining of paraffin sections of CT26 tumours 2 days after application of bacteria. Overview of the tumour and 40× magnification of PAS-positive areas at the border between viable rim and necrosis (black box indicates location of the magnified region in the overview and additional arrows show strongly PAS positive areas).

*csgD,* yielding SL7207Δ*csgD* and the corresponding complemented strain SL7207Δ*csgD-c*. Bacterial strains were grown in Luria–Bertani (LB) medium supplemented with 30 µg ml$^{-1}$ streptomycin at 37°C with shaking at 180 r.p.m.

### *Biofilm plates*

To confirm biofilm formation of *S. typhimurium in vitro*, biofilm plates containing LB medium without $NaCl_2$, Congo red (Serva) and Calcofluor (Sigma, Germany) were used (Römling *et al.*, 1998). Bacteria were grown first 24 h at 37°C and subsequently for 5 days at 30°C.

### *Cell lines and animals*

Six-week-old, female BALB/c mice were purchased from Janvier (France). CT26 colon carcinoma cells (ATCC CRL-2638) were grown as monolayers in IMDM Medium (Gibco BRL, Germany)

supplemented with 10% (v/v) heat-inactivated fetal calf serum (Integro, The Netherlands), 250 μmol $l^{-1}$ β-Mercaptoethanol (Serva) and 1% (v/v) penicillin/streptomycin (Sigma, Germany).

### *Infection of CT26 cells* in vitro

Cultured CT26 cells were transferred to a 24-well plate with coverslips and grown over night. Bacteria were added at a moi of 100 and spun down onto the cells for 1 min with 1000 r.p.m. After 1 h incubation at 37°C and 5% $CO_2$, medium was exchanged and gentamicin was added at a concentration of 50 μg $ml^{-1}$. After 2 h of incubation cells were washed twice with PBS and glass slides were either taken for confocal microscopy or cells were lysed and lysates were plated on LB agar plates supplemented with streptomycin to estimate intracellular bacteria.

### *Infection of tumour bearing mice*

Six-week-old, female BALB/c mice were subcutaneously injected with $5 \times 10^5$ CT26 cells at the abdomen. When the tumours had reached a size of 5–8 mm diameter, mice were injected intravenously with $5 \times 10^6$ colony-forming units (cfu) of *S. typhimurium* in phosphate-buffered saline solution (PBS). Two days p.i., mice were sacrificed, and tumour and spleen were removed for further analysis.

All animal experiments have been performed with the permission of the local authorities (LAVES) according to the animal welfare act.

### *Neutrophil depletion*

The neutrophil granulocytes were depleted by injecting tumour bearing mice for three consecutive days with 25 μg monoclonal rat-anti-Gr1 (RB6-8C5) antibody (day-1; 0; 1 p.i.). Blood samples were taken and analysed via flow cytometry to control the extend of depletion.

### *RNA preparation*

RNA of strain SL7207 was isolated from fixed samples with the RNeasy mini Kit (Qiagen) according to the manufacturer's instructions using the double amount of buffers when appropriate. For RNA preparation of bacterial RNA from infected tumour tissue the tumours were cut into small pieces and the necrotic tissue was squeezed through a cell strainer, 70 μm (BD Falcon) in presence of 3 ml RNA protect bacteria reagent (Ambion). For RNA isolation of bacterial RNA from infected spleen tissue, the organs were homogenized with a tissue homogenizer in presence of 2 ml RNA protect bacteria reagent on ice. The samples were centrifuged briefly at 1000 r.p.m. to separate the bacteria from tissue debris following a centrifugation step at maximum speed for 5 min to pellet the bacteria. RNA quality was accessed using the Agilent 2100 Bioanalyzer.

### *RT-qPCR analysis*

cDNA was prepared from RNA using the RevertAid First Strand cDNA synthesis Kit (Fermentas) according to the instructions of the manufacturer. RT-qPCRs were carried out with the Power Sybr Green PCR Master Mix (Applied Biosystems) and an 7500 Real-Time PCR System (Applied Biosystems), and the data were analysed by the Sequence Detection Software, version 1.4 (Applied Biosystems), according to manufacturer's specifications. Measured values of the biofilm genes were normalized to the housekeeping gene *gyrB*. Normalized values were used to calculate the ratios of the expression.

### *Real-time PCR*

To the samples, containing 2 μg RNA, 4 μl 5× Buffer (Fermentas), 1 μl DNase (Qiagen) and DEPC-treated water (Fermentas) were added to an overall volume of 20 μl. After 15 min incubation at 37°C and 10 min at 65°C, the samples were chilled on ice. Subsequently, 10 μl of the RNA mix was equipped with 1 μl random hexamers (0.2 μg $\mu l^{-1}$, Fermentas) and 1 μl DEPC-treated water (Fermentas) and incubated at 70°C for 5 min. After cooling down, 3 μl DEPC-treated water, 2 μl $5 \times 1$ strand buffer (Fermentas), 2 μl 10 mM dNTP mix (Fermentas) and 1 μl Ribonuclease inhibitor (20 u $\mu l^{-1}$, Fermentas) were added. Before adding 1 μl M-MuLV-RT (Fermentas) the samples were incubated at 25°C for 5 min. The program for reverse transcription proceeded under the following conditions: 10 min incubation at 25°C, 1 h at 42°C and 10 min at 70°C. After chilling on ice, 80 μl DEPC-treated water was added and the samples used for PCR. The PCR mix contained the following ingredients: 2 μl 10× Taq Buffer (Biotherm), 0.5 μl dNTPs (10 mM), 2 μl Primermix (10 mM), 15.5 μl $H_2O$, 1 μl cDNA and 0.1 μl Taq (Biotherm). The PCR was performed using the following conditions: 95°C for 2 min, 35 cycles with 95°C, 60°C and 72°C each for 30 s and additionally 72°C for 5 min. Samples were examined on a 2% agarose gel.

### *Transmission electron microscopy*

Tumours were fixed in 5% formaldehyde and 2% glutaraldehyde and cut into cubes with a length of 3–5 mm. Subsequently, the samples were contrasted in 1% aqueous osmium tetroxide and dehydrated with a graded series of acetone (10%, 30%, 50%, 70%, 90%, 100%) on ice for 30 min per step. The dehydrated samples were infiltrated with an epoxy-embedding resin (Spurr, 1969) (1 part acetone/1 part resin; 1 part acetone/2 parts resin, pure resin alternating). The infiltrated samples were polymerized at 70°C for 10 h and cut into ultrathin section with a diamond knife. The sections were picked up with formvar-coated-grids and contrasted with uranylacetate and lead-citrate. Finally, the samples were analysed using a transmission electron microscope (TEM910 Zeiss, Germany) at an acceleration voltage of 80 kV.

### *Scanning electron microscopy*

Again, tumours were fixed in 5% formaldehyde and 2% glutaraldehyde in cacodylate buffer followed by three times washing in cacodylate buffer (0.1 M cacodylate; 0.01 M $CaCl_2$; 0.01 M $MgCl_2$; 0.09 M saccharose; pH 6.9). Subsequently, the samples were dehydrated with a graded series of acetone (10%, 30%, 50%, 70%, 90%, 100%) on ice for 30 min per step. After a double wash with 100% acetone at RT for 30 min, the samples were

dried with liquid $CO_2$ and fixed between sample brackets. By uncompressing the brackets, the samples were broken. The fractured surface was sputtered with a thin gold layer. Finally, the samples were analysed with a Zeiss field emission scanning electron microscope DSM 982 Gemini at an acceleration voltage of 5 kV. Images were digitally stored on MO-disks. Images were recorded digitally with a Slow-Scan CCD-Camera (ProScan, $1024 \times 1024$, Scheuring, Germany) with ITEM-Software (Olympus Soft Imaging Solutions, Münster, Germany).

### *Histology*

For the preparation of paraffin section tumours were fixed in 10% (v/v) paraformaldehyde. After embedding in paraffin wax sections with a thickness of 5 μm they were placed on Starfrost slides and stained with a periodic acid-schiff (PAS) stain. The stained sections were analysed with an Olympus BX51 microscope and pictures were taken with an Olympus U-CMAD3 camera using the software ZEN 2009.

## Acknowledgements

The authors wish to thank Susanne zur Lage, Regina Lesch and Ina Schleicher for expert technical assistance. This work was supported in part by the Deutsche Krebshilfe, the Ministry of Education and Research (BMBF) and the German Research Council (DFG).

## References

Avogadri, F., Martinoli, C., Petrovska, L., Chiodoni, C., Transidico, P., Bronte, V., *et al*. (2005) Cancer immunotherapy based on killing of *Salmonella*-infected tumor cells. *Cancer Res* **65:** 3920–3927.

Coley, W.B. (1893) The treatment of malignant tumors by repeated inoculations of erysipelas. With a report of ten original cases. *Am J Med Sci* **105:** 487–511.

Crawford, R.W., Rosales-Reyes, R., Ramirez-Aguilar, M.L., Chapa-Azuela, O., Alpuche-Aranda, C., and Gunn, J.S. (2010) Gallstones play a significant role in *Salmonella* spp. gallbladder colonization and carriage. *Proc Natl Acad Sci USA* **107:** 4353–4358.

Cunningham, C., and Nemunaitis, J. (2001) A phase I trial of genetically modified *Salmonella typhimurium* expressing cytosine deaminase (TAPET-CD, VNP20029) administered by intratumoral injection in combination with 5-fluorocytosine for patients with advanced or metastatic cancer. *Protocol no: CL-017. Version: April 9, 2001*. *Hum Gene Ther* **12:** 1594–1596.

Datsenko, K.A., and Wanner, B.L. (2000) One-step inactivation of chromosomal genes in *Escherichia coli* K-12 using PCR products. *Proc Natl Acad Sci USA* **97:** 6640–6645.

Dickschat, J.S. (2010) Quorum sensing and bacterial biofilms. *Nat Prod Rep* **27:** 343–369.

Ebbell, B. (1937) *The Papyrus Ebers: The Greatest Egyptian Medical Document*. London: Oxford Press.

Flemming, H.C., and Wingender, J. (2010) The biofilm matrix. *Nat Rev Microbiol* **8:** 623–633.

Gerstel, U., and Römling, U. (2003) The *csgD* promoter, a control unit for biofilm formation in *Salmonella typhimurium*. *Res Microbiol* **154:** 659–667.

Grantcharova, N., Peters, V., Monteiro, C., Zakikhany, K., and Römling, U. (2010) Bistable expression of CsgD in biofilm development of *Salmonella enterica* serovar *typhimurium*. *J Bacteriol* **192:** 456–466.

Gualdi, L., Tagliabue, L., and Landini, P. (2007) Biofilm formation-gene expression relay system in *Escherichia coli*: modulation of sigmaS-dependent gene expression by the CsgD regulatory protein via sigmaS protein stabilization. *J Bacteriol* **189:** 8034–8043.

Hall-Stoodley, L., and Stoodley, P. (2005) Biofilm formation and dispersal and the transmission of human pathogens. *Trends Microbiol* **13:** 7–10.

Hoiby, N., Bjarnsholt, T., Givskov, M., Molin, S., and Ciofu, O. (2010) Antibiotic resistance of bacterial biofilms. *Int J Antimicrob Agents* **35:** 322–332.

Hoiseth, S.K., and Stocker, B.A. (1981) Aromatic-dependent *Salmonella typhimurium* are non-virulent and effective as live vaccines. *Nature* **291:** 238–239.

Hoption Cann, S.A., van Netten, J.P., and van Netten, C. (2003) Dr William Coley and tumour regression: a place in history or in the future. *Postgrad Med J* **79:** 672–680.

Jonas, K., Tomenius, H., Kader, A., Normark, S., Romling, U., Belova, L.M., and Melefors, O. (2007) Roles of curli, cellulose and BapA in *Salmonella* biofilm morphology studied by atomic force microscopy. *BMC Microbiol* **7:** 70.

Lahiri, A., Lahiri, A., Iyer, N., Das, P., and Chakravortty, D. (2010) Visiting the cell biology of *Salmonella* infection. *Microbes Infect* **12:** 809–818.

Lehrer, R.I. (2004) Primate defensins. *Nat Rev Microbiol* **2:** 727–738.

Leschner, S., and Weiss, S. (2010) *Salmonella*-allies in the fight against cancer. *J Mol Med* **88:** 763–773.

Leschner, S., Westphal, K., Dietrich, N., Viegas, N., Jablonska, J., Lyszkiewicz, M., *et al*. (2009) Tumor invasion of *Salmonella enterica* serovar Typhimurium is accompanied by strong hemorrhage promoted by TNF-alpha. *PLoS ONE* **4:** 6692.

Loessner, H., Endmann, A., Leschner, S., Westphal, K., Rohde, M., Miloud, T., *et al*. (2007) Remote control of tumour-targeted *Salmonella enterica* serovar Typhimurium by the use of L-arabinose as inducer of bacterial gene expression *in vivo*. *Cell Microbiol* **9:** 1529–1537.

Loussert, C., Schmitt, C., Prevost, M.C., Balloy, V., Fadel, E., Philippe, B., *et al*. (2010) *In vivo* biofilm composition of *Aspergillus fumigatus*. *Cell Microbiol* **12:** 405–410.

McBain, A.J. (2009) Chapter 4: *in vitro* biofilm models: an overview. *Adv Appl Microbiol* **69:** 99–132.

Römling, U. (2005) Characterization of the rdar morphotype, a multicellular behaviour in Enterobacteriaceae. *Cell Mol Life Sci* **62:** 1234–1246.

Römling, U., and Rohde, M. (1999) Flagella modulate the multicellular behavior of *Salmonella typhimurium* on the community level. *FEMS Microbiol Lett* **180:** 91–102.

Römling, U., Bian, Z., Hammar, M., Sierralta, W.D., and Normark, S. (1998) Curli fibers are highly conserved between *Salmonella typhimurium* and *Escherichia coli* with respect to operon structure and regulation. *J Bacteriol* **180:** 722–731.

Römling, U., Rohde, M., Olsen, A., Normark, S., and Reinkoster, J. (2000) AgfD, the checkpoint of multicellular and aggregative behaviour in *Salmonella typhimurium* regulates at least two independent pathways. *Mol Microbiol* **36:** 10–23.

Royo, J.L., Becker, P.D., Camacho, E.M., Cebolla, A., Link, C., Santero, E., and Guzman, C.A. (2007) *In vivo* gene regulation in *Salmonella* spp. by a salicylate-dependent control circuit. *Nat Methods* **4:** 937–942.

Scher, K., Romling, U., and Yaron, S. (2005) Effect of heat, acidification, and chlorination on *Salmonella enterica* serovar *typhimurium* cells in a biofilm formed at the air-liquid interface. *Appl Environ Microbiol* **71:** 1163–1168.

Shirtliff, M.E., Mader, J.T., and Camper, A.K. (2002) Molecular interactions in biofilms. *Chem Biol* **9:** 859–871.

Simm, R., Lusch, A., Kader, A., Andersson, M., and Römling, U. (2007) Role of EAL-containing proteins in multicellular behavior of *Salmonella enterica* serovar Typhimurium. *J Bacteriol* **189:** 3613–3623.

Spurr, A.R. (1969) A low-viscosity epoxy resin embedding medium for electron microscopy. *J Ultrastruct Res* **26:** 31–43.

Stepanovic, S., Cirkovic, I., Ranin, L., and Svabic-Vlahovic, M. (2004) Biofilm formation by *Salmonella* spp. and *Listeria* monocytogenes on plastic surface. *Lett Appl Microbiol* **38:** 428–432.

Stritzker, J., Weibel, S., Seubert, C., Gotz, A., Tresch, A., van Rooijen, N., *et al*. (2010) Enterobacterial tumor colonization in mice depends on bacterial metabolism and macrophages but is independent of chemotaxis and motility. *Int J Med Microbiol* **300:** 449–456.

Westphal, K., Leschner, S., Jablonska, J., Loessner, H., and Weiss, S. (2008) Containment of tumor-colonizing bacteria by host neutrophils. *Cancer Res* **68:** 2952–2960.

White, A.P., Gibson, D.L., Collinson, S.K., Banser, P.A., and Kay, W.W. (2003) Extracellular polysaccharides associated with thin aggregative fimbriae of *Salmonella enterica* serovar enteritidis. *J Bacteriol* **185:** 5398–5407.

White, A.P., Gibson, D.L., Kim, W., Kay, W.W., and Surette, M.G. (2006) Thin aggregative fimbriae and cellulose enhance long-term survival and persistence of *Salmonella*. *J Bacteriol* **188:** 3219–3227.

Yu, Y.A., Shabahang, S., Timiryasova, T.M., Zhang, Q., Beltz, R., Gentschev, I., *et al*. (2004) Visualization of tumors and metastases in live animals with bacteria and vaccinia virus encoding light-emitting proteins. *Nat Biotechnol* **22:** 313–320.

## Supporting information

Additional Supporting Information may be found in the online version of this article:

**Fig.S 1.** *In vitro* infection of CT26 cells with SL7207.
A. Z-Stack of confocal microscopic images of infected CT26 tumour cells *in vitro* 2 h after infection.
B. Gentamicin protection assay. Colony numbers of parental SL7207 were set as100% and used to normalize cfu of the other strains.
**Fig. S2.** Transmission electron micrographs of CT26 tumours 2 days post infection. Magnification of electron micrographs of Fig. 5.
**Fig. S3.** PAS staining of paraffin sections of CT26 tumours 2 days after application of bacteria. Magnification of PAS-staining of infected tumours of Fig. 6.
**Fig. S4.** Efficiency of tumour colonization and anti-tumour therapeutic potential of mutants lacking the ability to form biofilms.
A. Kinetic of tumour and organ colonization by parental SL7207 as well as *ΔadrA* and *ΔcsgD* variants. Bars represent mean of tumours from 5 mice ± SDM.
B. Tumour growth after application of parental SL7207 or *ΔadrA*/*ΔcsgD* mutants. Tumour size of individual mice per group is given as percent of tumour size on day 2.

Please note: Wiley-Blackwell are not responsible for the content or functionality of any supporting materials supplied by the authors. Any queries (other than missing material) should be directed to the corresponding author for the article.